doi: 10.17221/6/2017-CJAS

# Effect of Melatonin from Slow-Release Implants on Aquaporins (AQP1 and AQP4) in the Ovine Choroid Plexus

*Aleksandra Szczepkowska[1], Mariusz Tomasz Skowroński[2,3], Marta Kowalewska[1], Stanisław Milewski[4], Janina Skipor[1]**

[1]*Institute of Animal Reproduction and Food Research, Polish Academy of Sciences, Olsztyn, Poland*

[2]*Department of Animal Physiology, Faculty of Biology and Biotechnology, University of Warmia and Mazury in Olsztyn, Olsztyn, Poland*

[3]*Institute of Veterinary, Poznań University of Life Sciences, Poznań, Poland*

[4]*Department of Sheep and Goat Breeding, Animal Bioengineering Faculty, University of Warmia and Mazury in Olsztyn, Olsztyn, Poland*

**Corresponding author: j.skipor@pan.olsztyn.pl*

**ABSTRACT**

Szczepkowska A., Skowroński M.T., Kowalewska M., Milewski S., Skipor J. (2018): **Effect of melatonin from slow-release implants on aquaporins (AQP1 and AQP4) in the ovine choroid plexus**. Czech J. Anim. Sci., 63, 32–42.

Aquaporins (AQPs) play important role in the cerebrospinal fluid (CSF) secretion and AQP1 and AQP4 are localized in the choroid plexus (CP), which is the main place of CSF production. In ewes, seasonally breeding animals, the turnover rate (TOR) of CSF is photoperiodically modulated and melatonin, a biochemical signal about changing photoperiod, is used to advance the onset of the breeding season by mimicking the stimulatory effect of short days (SD). This study evaluates the effect of melatonin implantation during long days (LD) on AQPs expression in the ovine CP. Studies were performed on ovariectomized, estradiol implanted ewes treated with placebo ($n$ = 6) or with melatonin ($n$ = 6) during LD. Ewes were sacrificed 40 days after melatonin/placebo implantation and CPs from the lateral/third brain ventricles were collected for Real-time and Western blot analyses. Additionally, for immunohistochemical analysis, CP samples were collected from ewes ($n$ = 3) sacrificed during LD. We demonstrated an apical membrane localization of AQP1 and a diffused distribution of AQP4 in the epithelial cells of CP. The mRNA expression of *AQP1* was 20 times higher than the expression of all *AQP4* isoforms, and among them *AQP4* isoforms containing exon 2 constituted approximately 38%. The melatonin implantation significantly ($P < 0.05$) increased the mRNA expression of *AQP1* and *AQP4* and the protein level of AQP4 isoforms (33 and 28 kDa). For AQP1 we observed a significant ($P < 0.05$) decrease of glycosylated (33 kDa) and a significant ($P < 0.05$) increase of unglycosylated (23 kDa) predominant protein form. Therefore it can be suggested that at least AQP1, which is involved in CSF production and has been demonstrated to be modulated by melatonin implantation, is linked with the photoperiodic modulation of the CSF production in ewes.

**Keywords**: AQPs brain location; mimicked short days; cerebrospinal fluid; photoperiod; ewe

Supported by the National Science Centre of Poland (grant No. 2012/05/N/NZ9/01340) and by statutory research funds of the Ministry of Higher Education, Poland (immunohistochemical studies).

doi: 10.17221/6/2017-CJAS

**List of abbreviations**: CFS = cerebrospinal fluid, CP = choroid plexus, TOR = turnover rate, SD = short days, LD = long days, VEGF = vascular endothelial growth factor, VEGFR2 = vascular endothelial growth factor receptor 2, NRP1 = neuropilin 1, AQPs = aquaporins, MW = molecular weight, PB = phosphate buffer, BSA = bovine serum albumin, RT = reverse transcription, E2 = oestradiol

The cerebrospinal fluid (CSF) is a major part of extracellular fluid of the central nervous system, constantly produced mainly by choroid plexuses (CPs) of the brain ventricles, which are formed by tightly connected epithelial cells surrounding a core in which blood vessels are fenestrated (Skipor and Thiery 2008). This provides access of the blood-born substances to the immediate vicinity of tightly connected epithelial cells, forming blood-CSF barrier. It has been demonstrated that in ewes, access of progesterone, estradiol, and leptin to the CSF increases under long days (Thiery et al. 2003, 2006; Adam et al. 2006). These photoperiod-driven changes in the CSF steroid concentration are regulated through an unknown pineal-dependent mechanism (Thiery et al. 2006). The pineal gland is the main source of melatonin, a biochemical signal of daily rhythm and changing photoperiod which is released into the CSF and venous blood during the darkness. So far a few mechanisms have been suggested to explain photoperiod-driven changes in the CSF steroid concentration. The first, based on the discovery that in ewes the turnover rate (TOR) of CSF is higher during short days (SD) than long days (LD) (Thiery et al. 2009), considers variations in the CSF secretion rate with photoperiod, which would result in dilution or concentration of hormone molecules. The second one is connected with photoperiodic changes in blood–CSF permeability due to the higher expression of some tight junction proteins in the CPs during SD then LD (Lagaraine et al. 2011). Just recently we have demonstrated up-regulation of vascular endothelial growth factor (VEGF) receptor 2 (VEGFR2) and its co-receptor neuropilin 1 (NRP-1) by short photoperiod in the ovine CPs (Szczepkowska et al. 2012). We suggested that the VEGF-system, being involved in maintaining the fenestrated structure of microvessels in the CPs capillaries, may be engaged in photoperiodic plasticity of CP capillaries and therefore be responsible for photoperiodic changes in the CSF TOR in ewes (Szczepkowska et al. 2012).

The CSF secretion involves regulated transport of $Na^+$, $Cl^-$, and $HCO_3^-$ from the blood to the ventricles, creating an osmotic gradient driving the transcellular secretion of water through water channels – aquaporins (AQPs) (Nazari et al. 2015). AQPs, small integral membrane proteins (molecular weight (MW) ~30 kDa) constitute a ten-member family of water channels which play a major role during water transport in the kidney, brain secretory epithelia, and other organs (Agre et al. 2002). From this family, AQP1, AQP4, AQP5, AQP9, and AQP11 have been identified in the central nervous system (King and Agre 1996; Nazari et al. 2015). AQP4 and AQP1 play vital roles in the dynamic regulation of brain water homeostasis and the regulation of CSF production (Venero et al. 2001). The expression of both AQPs has been detected in the CPs. AQP1 is abundant on the apical (CSF-facing) surface of rat CPs from the fourth and lateral ventricles (Nielsen et al. 1993; Speake et al. 2003), therefore during the CSF secretion it plays a major role in mediating water transport across the apical membrane (Oshio et al. 2005). The mRNA for *AQP4* was initially detected in rat CPs from lateral ventricles, using the hybridization *in situ* method (Venero et al. 1999), thereafter also AQP4 protein was detected as diffusely distributed throughout the epithelial cells of rat CPs from the fourth and lateral ventricles (Speake et al. 2003; Nazari et al. 2015). It has been demonstrated that in rats the expression of AQP4 protein in astrocytes and AQP1 protein in spinal cord may be modulated by melatonin (Kaur et al. 2006; Nesic et al. 2008). It has not been known so far whether melatonin affects the AQPs expression in CP. Therefore the aim of the present study was to test the hypothesis that melatonin may increase the expression of AQPs in the ovine CP associated with an increase of water secretion during SD, the both being under the influence of melatonin or photoperiod. To test this we implanted ewes during LD with slow-release implants of melatonin (commonly used to advance the onset of a breeding season in seasonally breeding animals) that prolong duration of melatonin action and therefore mimic the physiological effect of SD (Chemineau et al. 1992). This model allows to evaluate the effect of

doi: 10.17221/6/2017-CJAS

melatonin (very low daytime melatonin concentration in LD ewes vs high daytime melatonin in LD melatonin-implanted ewes) and photoperiod (natural LD vs mimicked SD). Additionally we evaluated the localization of AQPs in the ovine CP using the immunocytochemistry method.

## MATERIAL AND METHODS

***Animals and treatment***. All experiments were conducted in accordance with the Polish Guide for the Care and Use of Animals and approved by the Local Ethics Committee. Based on our hypothesis that melatonin could act on AQPs in ovine CP, we decided to use the previous validated model of melatonin implanted ewes to mimic SD during the LD period (Chemineau et al. 1992). Studies were performed on female Blackheaded Mutton Sheep ($n$ = 12, 3–5 years old, body condition score 2.5) maintained indoors under natural lighting conditions and fed a constant diet of hay, straw, and commercial concentrates, with water and mineral licks available *ad libitum*. At the beginning of May (seasonal anoestrus) all ewes were ovariectomized and subcutaneously implanted with an oestradiol (E2) implant that maintained plasma E2 concentrations of 2–4 pg/ml (Thiery et al. 2006). In the middle of May, ewes were implanted with a melatonin slow-release implant Melovine (Ceva Sante Animale, France) ($n$ = 6, 18 mg of melatonin per implant) or sham-implanted ($n$ = 6) for approximately 40 days (from May 15$^{th}$ till June 25$^{th}$). On the day of experiment ewes were implanted with the jugular vein catheter in the morning and were placed in individual cages where they could lie down and have access to hay and water. To prevent the stress of social isolation, all ewes had visual contact. Blood samples were collected during the day through jugular vein venipuncture (one month after melatonin implantation) for melatonin measurement and through a catheter inserted into the jugular vein by every 30 min for 3 h before scarification (interval: 9:00–16:00 h) for prolactin measurement. Animals were killed between 12:00–16:00 h, by a licensed butcher and ewes were decapitated and CPs from the lateral/third ventricles were promptly collected from the dissected brains. Tissues were immediately frozen in liquid nitrogen and were stored at –80°C until use. The collected tissues were analyzed using Western blot and Real-time PCR methods. Additionally, three ewes were sacrificed during LD and CP samples for immunohistochemical analysis were obtained.

***Immunohistochemistry***. Immediately after decapitation, the brains of the three additionally sacrificed LD ewes were fixed via perfusion through both carotids with 1 l of 1% sodium nitrite in 0.9% saline, followed by perfusion with 3 l of fixative containing 4% paraformaldehyde in 0.1 M phosphate buffer (PB), pH 7.4. After dissection, CP from the lateral ventricles were collected and maintained in 0.1 M PB (pH 7.4) at 4°C. The tissue was dehydrated in ethanol followed by xylene and was finally embedded in paraffin; tissue sections of a 2 µm thickness were prepared.

The sections were dewaxed and rehydrated as previously described (Skowronski et al. 2007). For immunoperoxidase labelling, endogenous peroxidase was blocked by the exposure to 0.5% $H_2O_2$ in absolute methanol for 10 min at room temperature (Skowronski et al. 2007). To reveal the antigens, sections were submerged in 1 mM Tris solution (pH 9.0) supplemented with 0.5 mM ethylene glycol-bis[β-aminoethyl ether]-N,N,N',N'-tetraacetic acid (EGTA) and were heated in a microwave oven at 650 W for 6 min and then at 350 W for 10 min. After the treatment, sections were left for 30 min in the buffer to cool. Nonspecific binding of IgG was prevented by incubating the sections in 50 mM $NH_4Cl$ for 30 min, followed by blocking in PBS supplemented with 1% bovine serum albumin (BSA), 0.05% saponin, and 0.2% gelatine. Sections were incubated overnight at 4°C with primary antibodies raised against rabbit polyclonals AQP1 (ab15080) and AQP4 (ab46182) (Abcam, UK; working dilution 1 : 800) diluted in PBS supplemented with 0.1% BSA and 0.3% Triton X-100. The sections were rinsed with PBS supplemented with 0.1% BSA, 0.05% saponin, and 0.2% gelatine and then incubated with a horseradish peroxidase-conjugated secondary antibody P448 (Dako (Agilent) USA; 1 : 200). Labelling was visualized via a 10-min exposure to 0.05% 3,3 diaminobenzidine tetrahydrochloride (DAB).

Fluorescence techniques were employed to double-labelling tissues (Skowronski et al. 2007). After an overnight incubation with the rabbit anti-AQP1 antibody as described above, the sections were incubated with a fluorescent secondary antibody (donkey anti-rabbit Molecular Probes

doi: 10.17221/6/2017-CJAS

Alexa Fluor 546; Thermo Fisher Scientific, USA). After washing (PBS for 3 × 10 min), sections were incubated overnight with a rabbit anti-AQP4 antibody, and the immunoreactivity was visualized by using a donkey anti-rabbit (Molecular Probes Alexa Fluor 488; Thermo Fisher Scientific) and 4',6-diamidino-2-phenylindole (DAPI; Thermo Fisher Scientific) in a 1 : 10 000 solution prepared from a 5 mg/ml stock solution. After a final wash in PBS for 3 × 10 min, the sections were mounted in glycerol supplemented with antifade reagent (*N*-propyl-galat). The microscopic evaluation was performed using an Olympus BX51 light and fluorescence microscope (Olympus, Japan). In addition, anti-AQP1 and anti-AQP4 antibodies preincubated with the immunizing peptides ab25381 and ab46181 (Abcam), respectively, prevented labelling.

***Gene expression assays.*** CP was removed from its anchor to Galen's vein, and a split was made along the mid-line, which separated the CP from each lateral ventricle. Half of the CP from each animal was cut into small pieces, and the frozen tissue was homogenized in RA1 lysis buffer from the NucleoSpin RNA kit (Macherey-Nagel GmbH & Co. KG., Germany) in Lysing Matrix D (MP Biomedicals, USA) with a FastPrep-24 instrument (MP Biomedicals). The total RNA was extracted with a NucleoSpin RNA kit (Marcherey-Nagel) including a DNA digest step for the elimination of a possible genomic DNA contamination, according to the manufacturer's instructions. The concentration and quality of RNA that was isolated from the CP tissue was determined using a NanoDrop (Thermo Fisher Scietific) and 1.2% agarose gel electrophoresis. One microgram of total RNA was saved for further use in reverse transcription (RT) reactions. RT reactions were performed with a DyNAmo cDNA synthesis kit (Thermo Fisher Scientific) according to the manufacturer's protocol. The resulting cDNA was stored at –20°C until further analysis.

Real time PCR analyses were performed with the ViiA 7 Real-Time PCR system (Applied Biosystems, USA) using a DyNAmo SYBR Green qPCR kit (Thermo Fisher Scientific). Specific primer pairs were designed to amplify *AQP1*, $AQP4_{\text{all isoforms}}$, $AQP4_{\text{exon2}}$ (according to Moe et al. (2008), *AQP4* isoforms containing exon 2 have possible function of water transport through plasma membrane), and succinate dehydrogenase A (*SDHA*) (reference gene) transcripts and were used according to the literature for *GAPDH* and *HDAC1* reference genes (Table 1). All primers were synthesized by Genomed (Poland). PCR-derived DNA fragments (*AQP1*, $AQP4_{\text{all isoforms}}$, $AQP4_{\text{exon2}}$, and *SDHA*) were separated by electrophoresis on 2% agarose gels supplemented with 0.01% ethidium bromide and were examined under UV light (Gel Logic100; KODAK, USA). *AQP1*, $AQP4_{\text{all isoforms}}$, $AQP4_{\text{exon2}}$, and *SDHA* PCR products were sequenced (Genomed) to confirm their specificity. Each Real-time PCR reaction well (20 µl) contained 3 µl of diluted RT product,

Table 1. Sequences of oligonucleotide primers used for real time PCR analyses

| Genes | Primers (5'→3') | Product size (bp) | Accession No./literature source |
|---|---|---|---|
| *AQP1* | F: TCCAGGACCACTGGATCTTCT<br>R: CACCCTGGAGTTGATGTCGT | 143 | NM_001009194.1 |
| $AQP4_{\text{all isoforms}}$ | F GGTGCACGTGATCGACATTG<br>R: ACTGAAGACAACACCTCTCCAG | 75 | NM_001009279.1 |
| $AQP4_{\text{exon2}}$ | F: ATTAGCATCGCCAAGGCTGT<br>R: TTCTGTGAACCGTGGTGACT | 145 | NM_001009279.1 |
| *SDHA** | F: AGACGTTCGACAGGGGAATG<br>R: GACGGGCTTGGAGTAATCGT | 182 | XM_004017097.1 |
| *HDAC1** | F: CTGGGGACCTACGGGATATT<br>R: GACATGACCGGCTTGAAAAT | 115 | Herman et al. (2014) |
| *GAPDH** | F: TGACCCCTTCATTGACCTTC<br>R: GATCTCGCTCCTGGAAGATG | 143 | Herman et al. (2010) |

*AQP1* = aquaporin 1, $AQP4_{\text{all isoforms}}$ = aquaporin 4-all isoforms, $AQP4_{\text{exon2}}$ = aquaporin 4-exon 2, *SDHA* = succinate dehydrogenase A, *HDAC1* = histone deacetylase 1, *GAPDH* = glyceralaldehyde-3-phosphate dehydrogenase, F = forward, R = reverse
*reference genes

doi: 10.17221/6/2017-CJAS

0.1 µM forward and reverse primers, and 10 µl of DyNAmo SYBR Green PCR master mix (Thermo Fisher Scientific). The following protocol was used: 95°C for 15 min for the hot start *Thermus brockianus* DNA polymerase, 35 cycles of 95°C for 10 s (denaturation), and 60°C for 1 min (annealing and extension). After the completion of the cycles, a final melting curve analysis under continuous fluorescence measurement was performed to evaluate the specific amplification. The results were analyzed with Real-time PCR Miner (http://www.miner.ewindup.info/version2), based on the algorithm that was developed by Zhao and Fernald (2005).

***Western blot analyses***. The second part of CP was cut into small pieces and was homogenized while still frozen in lysing MatrixD tubes (MP Biomedicals) with 500 µl of ice-cold lysis buffer consisting of 100 mM NaCl, 1% Triton X-100, 2 mM EDTA, 0.2% sodium dodecyl sulphate (SDS), 0.5% sodium deoxycholate, and 1% protease and phosphatase inhibitor cocktail (Thermo Fisher Scientific) and was homogenized in a FastPrep instrument (MP Biomedicals) at an oscillation speed of 6.5 for 30 s. Disruption was repeated 3 times, and between the cycles, samples were placed on ice. After the last cycle, tubes were briefly centrifuged at 5000 *g* to remove any undisrupted tissues. Homogenates were then transferred into new tubes and were centrifuged at 13 000 *g* for 30 min at 4°C. The supernatants were used for protein quantification using a Bradford kit (BIO-QUANT Protein; Merck Millipore, USA). Aliquots of 100 µg of protein were stored at –80°C until they were loaded on 12% SDS-polyacrylamide gels transferred to a 0.45 µm Immobilon P membrane (Merck Millipore) using a semi-dry technique (Trans-blot SD; BioRad Laboratories, USA). Molecular weight standards were included for each immunoblot. The membranes were then blocked with 5% non-fat milk in TBST (Tris-buffered saline with 0.5% Tween-20) buffer for 1.5 h at room temperature, extensively washed in TBST, and incubated overnight at 4°C with the appropriate primary antibody solution. The following primary antibodies were used: rabbit polyclonal anti AQP1 (ab15080, Abcam; working dilution 1 : 500) and AQP4 (ab46182, Abcam; working dilution 1 : 500). Next, immunoblots were incubated for 1.5 h at room temperature with goat anti-rabbit biotin-conjugated antibodies that were included in the WesternDot$^{TM}$ kit and were visualized with Qdot 625 streptavidin conjugate (Invitrogen by Life Technologies) according to the manufacturer's instructions. Then, the blots were examined under UV light (Gel Logic100, KODAK). The blots were stripped and re-probed with a rabbit polyclonal anti-GAPDH antibody conjugated to horseradish peroxidase (Santa Cruz Biotechnology, USA) as the protein loading control, which was then detected with the enhanced chemiluminescence SuperSignal West Dura Kit (Thermo Fisher Scientific) and imaged with the VersaDoc Imaging System (BioRad Laboratories). In addition, to confirm binding specificity, some blots were incubated with antibodies that were pre-adsorbed with excess amounts of their respective peptides (AQP1 – ab25381 and AQP4 – ab46181; Abcam).

***Melatonin and prolactin measurements***. The ability of the melatonin slow-release implants to maintain permanently high blood concentrations of melatonin and the effectiveness of these implants were monitored by determining diurnal melatonin and prolactin concentrations.

The concentraction of melatonin in the blood plasma was assayed, as a control of melatonin level in implanted ewes, according to the method of Fraser et al. (1983) that was modified by Misztal et al. (1996), using ovine anti-melatonin serum (Dr. A. Foldes, CSRIO, Australia). Synthetic melatonin (Sigma-Aldrich, USA) was used as a standard and [O-methyl-3H]-melatonin (Amersham PLC, UK) was used as a tracer. The sensitivity of the assay was 16.8 ± 8.0 pg/ml and the intra- and inter-assay coefficients of variation were 10.5% and 13.2%, respectively.

The level of prolactin was measured in blood plasma via the radioimmunoassay method described by Wolinska et al. (1977). The prolactin standard was kindly provided by Prof. Kazimierz Kochman from the Kielanowski Institute of Animal Physiology and Nutrition, Polish Academy of Sciences in Jablonna. The sensitivity of the assay was 2 ng/ml, and the intra- and inter-assay coefficients of variation were 9% and 12%, respectively.

***Data analysis***. The Real-time PCR results are presented as the relative gene expression of the target gene vs the three reference genes. The Western blot data are presented as the relative optical density of the target protein vs the loading control (*GAPDH*). All of the values that were obtained in Real-time PCR and Western blot analyses are pre-

doi: 10.17221/6/2017-CJAS

sented as the mean ± SEM for each group and were normalized to control group values, which were presented as 100%. Melatonin (pg/ml) and prolactin (ng/ml) concentrations are presented as the mean ± SEM for each group. The significance of differences between the results were assessed using the Mann-Whitney *U* test or one-way analysis of variance with multiple comparison of Tukey's *post-hoc* test (AQP profile only) (PRISM 6, Graph Pad), and a *P*-value of $< 0.05$ was regarded as statistically significant.

## RESULTS

***Immunohistochemistry.*** Immunohistochemical staining with polyclonal antibodies against AQP1 and AQP4 demonstrated the expression of both proteins in the epithelial cells of ovine CPs, whereas no staining was observed in negative control (Figure 1a). Distinct staining for AQP1 in the apical membrane of CP epithelium was observed via both immunoperoxidase and immunofluorescence labelling (Figure 1b and Figure 1d, e, respectively; indicated by arrowheads). Using both labelling methods, as described above, we showed that AQP4 is dispersed in the cytoplasm of CP epithelial cells (Figure 1c and Figure 1d, e, respectively; indicated by arrows). To examine protein co-localization, two fluorescence images of AQP1 (red) and AQP4 (green) were merged (Figure 1d, e).

***Plasma melatonin and prolactin concentrations.*** The mean (± SEM) daytime plasma concentration of melatonin in melatonin-implanted ewes reached 151 ± 56 pg/ml and was higher ($P < 0.05$) than in the control group where it amounted 4 ± 1 pg/ml. Before sacrification in late June, mean (± SEM) plasma prolactin concentration in melatonin-implanted ewes was lower ($P < 0.05$) compared to control ewes and reached 63 ± 27 ng/ml vs 146 ± 43 ng/ml, respectively.

***Impact of melatonin implantation on mRNA expression of AQPs.*** The pattern of *AQPs* mRNA expression in ovine CP is presented in Figure 2a. The expression of *AQP1* was approximately 20 times higher comparing to the expression of all isoforms of *AQP4*. Interestingly, the isoforms of *AQP4* containing the sequence of exon 2 represent only 38% of all *AQP4* isoforms expressed in the ovine CP. Melatonin

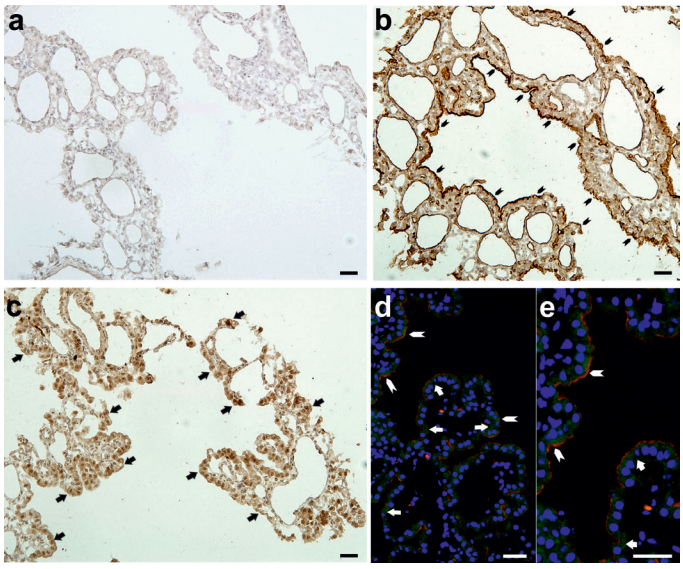


Figure 1. Immunoperoxidase and immunofluorescence signals indicate the localization of AQP1 and AQP4 in the ovine choroid plexus. No staining was observed with the use of non-immune immunoglobulins (**a** – negative control for immunoperoxidase). The AQP1 antibody was bound to the epithelial cells of the apical membranes of the choroid plexus (**b** and **d, e** – arrowheads indicate the apical membranes in immunoperoxidase and immunofluorescence labelled sections, respectively). AQP4 is diffusely expressed in the sheep choroid plexus epithelial cells (**c** and **d**, **e** – arrows show this localization in immunoperoxidase and immunofluorescence labelled sections, respectively). For immunofluorescence the choroid plexus tissue was stained for AQP1 (red) and AQP4 (green). The two fluorescence images were merged to demonstrate the localization of AQP1 (red) and AQP4 (green) (**d**, **e**). The blue signal in the images represents DAPI staining of nuclei. Bar = 20 μm

doi: 10.17221/6/2017-CJAS

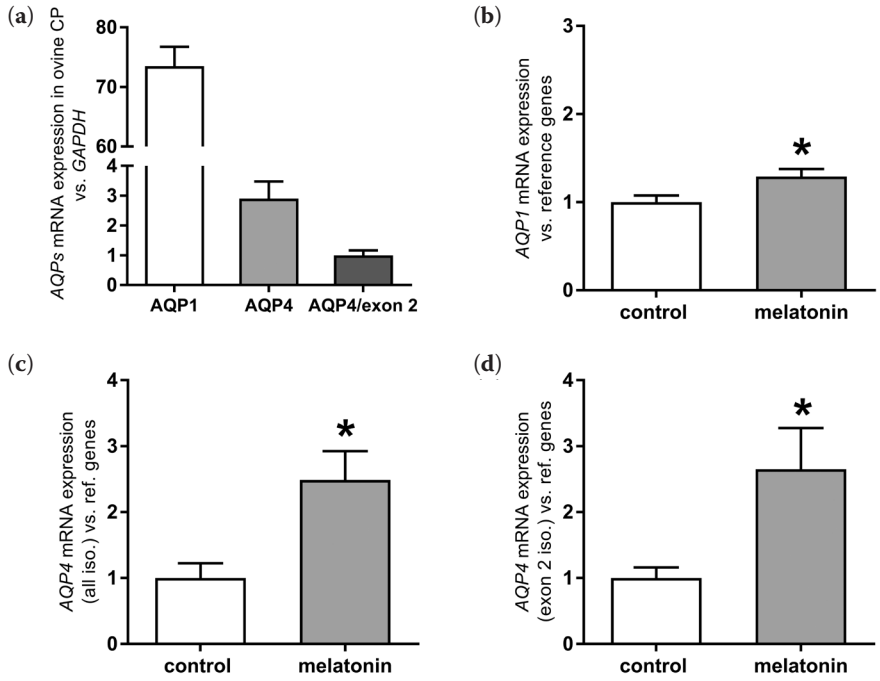


Figure 2. Effect of melatonin implantation on the mRNA expression of aquaporins. The mRNA expression of aquaporin 1 – *AQP1* (**b**), aquaporin 4 – *AQP4* for all isoforms (**c**) and *AQP4* for isoforms including exon 2 (**d**) were analyzed in the ovine choroid plexus (CP) samples that were obtained from the lateral/third ventricles of control (white bars, $n = 6$) and melatonin implanted (grey bars, $n = 6$) ewes. Bars indicate the mean (± SEM) relative expression of mRNA that was normalized to three reference genes (**b**–**d**). Additionally the profile of aquaporins expression in the ovine CP is shown (**a**) as the mean (± SEM) relative expression of mRNA of control groups ($n = 6$) that were normalized to *GAPDH* reference gene. Differences between means marked with asterisks or different letters are statistically significant ($P < 0.05$)

implantation significantly ($P < 0.05$) increased the *AQP1* mRNA expression (~29%, Figure 2b) as well as all *AQP4* isoforms and exon 2 *AQP4* isoforms (~150%, Figure 2c and Figure 2d, respectively).

***Impact of melatonin implantation on protein expression of AQPs.*** AQP1 Western blot analysis detected two specific bands of 33 kDa and 23 kDa in the ovine CP (Figure 3a). However, blocking of antibodies did not completely abolish the signal of 23 kDa, what may result from an insufficient amount of blocking peptide used. The relative abundance of these protein forms was as follows: 23 kDa > 33 kDa with a difference of about 40%. Melatonin implantation slightly, but significantly ($P < 0.05$) in-

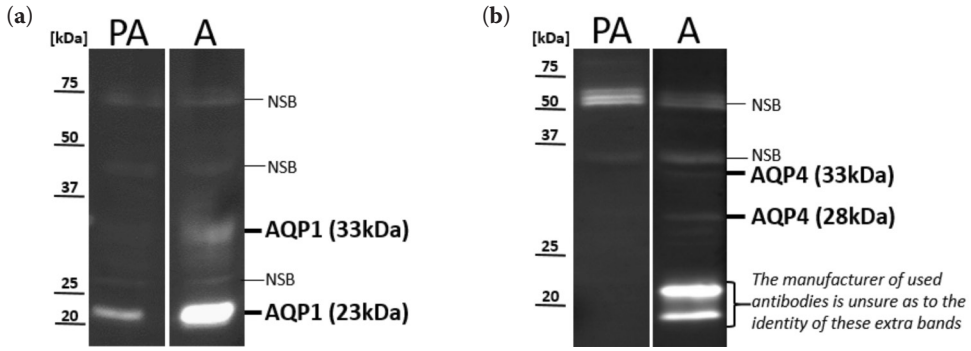


Figure 3. Specificity of the AQP1 (**a**) and AQP4 (**b**) antibodies in Western blot analyses of the ovine choroid plexus homogenates. Samples were probed with either free antibody or antibody pre-adsorbed with specific control peptides
A = antibodies, PA = pre-adsorbed antibodies, NSB = non-specific binding

doi: 10.17221/6/2017-CJAS

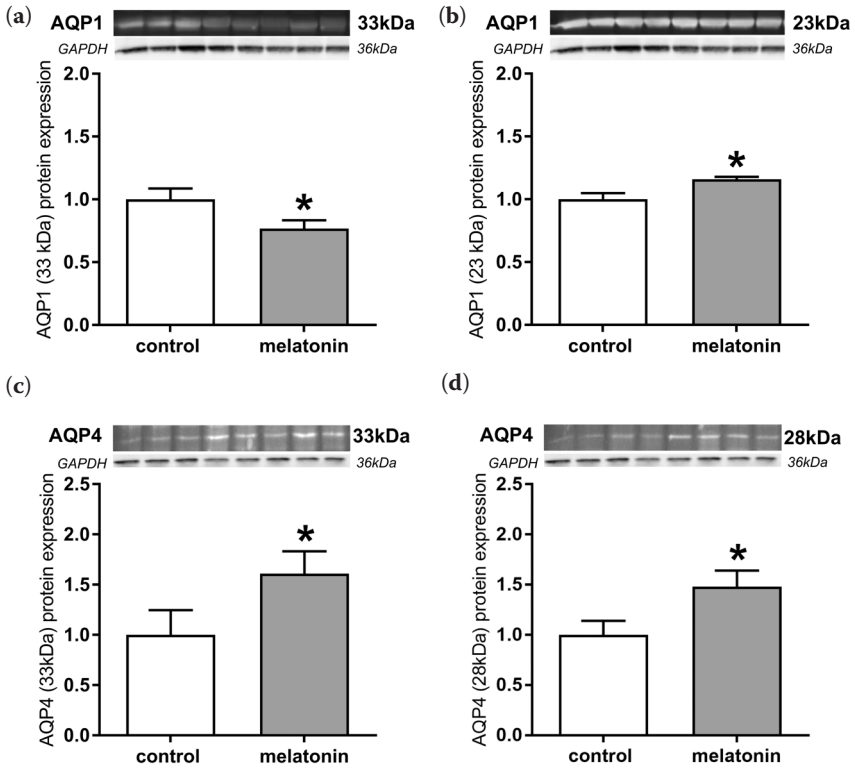


Figure 4. Effect of melatonin implantation on the protein expression of aquaporins. The protein level of AQP1 with approximately 33 kDa (**a**) and 23 kDa (**b**) of molecular weight (MW) and that of AQP4 with approximately 33 kDa (**c**) and 28 kDa (**d**) of MW were analyzed in the choroid plexus samples that were obtained from the lateral/third ventricles of control (white bars, $n = 6$) and melatonin implanted (grey bars, $n = 6$) ewes. Western immunoblots that contain 4 bands corresponding to each group are presented in the top panels. Bars indicate the mean (± SEM) relative optical density that was normalized to GAPDH as an internal control

Differences between means marked with asterisks are statistically significant ($P < 0.05$)

creased the level of 23 kDa AQP1 (~16%, Figure 4b) and decreased 33 kDa AQP1 (~24%, Figure 4a). The AQP4 antibody detected two specific bands of approximately 33 kDa and 28 kDa (Figure 3b). Despite that the blocking of antibodies completely abolished 2 additional bands on the level 23 and 17 kDa, we did not consider them as AQP4 according to manufacturer's suggestion. Melatonin implantation caused a significant increase in the expression of both AQP4 forms, 33 kDa (~60%) and 28 kDa (~48%) (Figure 4c and Figure 4d, respectively).

## DISCUSSION

In the current study we demonstrated the *AQP1* and *AQP4* mRNA and protein expression and their cellular localization in the ovine CP. The mRNA expression profile of *AQPs* in the ovine CP showed 20 times higher expression of *AQP1* compared to all isoforms of *AQP4.* AQP1 was found to be located almost exclusively in the apical membrane of the CP epithelium, which is in agreement with earlier studies that were conducted on rat CPs (Nielsen et al. 1993; Speake et al. 2003). This localization directly indicates the involvement of AQP1 in the transport of water through the apical membrane of the CP and, therefore, the involvement of AQP1 in CSF production (Owler et al. 2010). This is supported by previously demonstrated CSF production reduced by ~25% in AQP1 null mice compared to wild type mice (Oshio et al. 2005). Using Western blot we showed the presence of 33 and 23 kDa bands, which seems to be immunoreactive AQP1 protein, since their signals were completely or mostly blocked through using pre-adsorbed antibodies. Our results are similar to that obtained by Nesic et al. (2008) demonstrating the presence of fuzzy band of 37 kDa in cytosolic fraction and 24 kDa band in the membrane fraction of rat spi-

doi: 10.17221/6/2017-CJAS

nal cord. On the other hand, Nazari et al. (2015) observed 32 and 27 kDa immunoreactive bands in the rat CP. According to Nielsen et al. (1993) these bands may correspond with glycosylated and unglycosylated forms of AQP1, respectively. The localization of AQP4 in the ovine CP, which can be characterized as diffuse in the cytoplasm of epithelial cells, is in line with the findings of Speake et al. (2003) and Nazari et al. (2015). It has been demonstrated that rat *AQP4* has six cDNA isoforms which are differentially expressed in the kidney and brain (Moe et al. 2008). Three isoforms have exon 2, membrane localization, and transport water (Neely et al. 1999) while other three isoforms do not contain exon 2, have intracellular localization, and do not transport water (Moe et al. 2008). According to Moe et al. (2008) exon 2 may be responsible for cellular sorting of *AQP4*, since *AQP4* isoforms lacking exon 2 retained in the *cis*-Golgi instead being transported to the plasma membrane. Moreover, it has been suggested that the lack of exon 2 may be responsible for a loss of water transport capacity of *AQP4*. So far, little is known about isoforms of ovine *AQP4*. In our study we used two different primer pairs for *AQP4* what allowed us to analyze the expression of all isoforms and isoforms that contain exon 2. We observed that mRNA of *AQP4* isoforms, which contain exon 2, constitute only 38% of all *AQP4* isoforms expressed in the ovine CP. This stays in line with our immunohistochemistry analysis demonstrating *AQP4* localization mainly in the cytoplasm. Antibodies used in both, immunohistochemistry and Western blot method, were manufactured using peptide the sequence of which is entirely located in exon 1 being present in all known isoforms of *AQP4* (Moe et al. 2008). Indeed, we observed 33 kDa and 28 kDa immunoreactive AQP4 bands that may represent different AQP4 isoforms, these located in the membrane and in the cytoplasm. The closed molecular weights of AQP4 related bands (31 and 32 kDa) were observed by Ron et al. (2005) in the ovine cerebral cortex. Moreover, these authors suggested that the two obtained bands may be associated with subtypes of AQP4 or glycosylated/anglycosylated form of this protein. The involvement of AQP4 in choroidal CSF production is not clear. Data demonstrating reduction in CSF production in most of the *AQP4*-null compared to the wild-type mice (Li et al. 2009) indicate a role of AQP4 in water transfer in the CP. On the other hand, the cytoplasmic localization of AQP4 rather excludes its role as a water channel. Therefore, further studies are necessary to evaluate the presence of different *AQP4* isoforms in the CP.

The present study is the first to report on the effect of melatonin from slow-release implants, mimicking SD, on AQP1 and AQP4 expression in the ovine CP. The melatonin implantation during the natural long-day period (May–June) caused an elevation of *AQP1* and *AQP4* mRNA expression. Moreover we observed an increase of AQP4 and unglycosylated form of AQP1 proteins. Melatonin implantation reduced the level of glycosylated form of AQP1 protein. These results, therefore, confirmed our hypothesis that melatonin increases AQPs in the ovine CP associated with an increase of water secretion during SD, the both being under the influence of melatonin or photoperiod. There are no available data about the direct impact of melatonin on AQPs in the CP in physiological conditions. However, we know that melatonin has a potential to act directly on the ovine CP through its receptors MT1 and MT2 (Coge et al. 2009). Moreover, because melatonin significantly decreased cortisol plasma concentration in socially isolated ewes (Guesdon et al. 2013) and corticosteroids (dexamethasone) pretreatment reduced the expression of AQP4 protein in the ovine cerebral cortex (Ron et al. 2005), we considered also the potential effect of stress. The concentration of cortisol in blood plasma of sheep used in our experiment was measured and results were published by Kowalewska et al. (2017). The similar low levels of cortisol demonstrated in blood plasma of control (10.8 ± 1.9 ng/ml) and melatonin-implanted (10.9 ± 1.2 ng/ml) ewes rather exclude the cortisol effect. Considering the lower prolactin concentrations in the melatonin-implanted ewes compared to the control ewes, we confirmed that in the present study, melatonin implanted ewes resembled ewes in the SD period. In ewes, a low level of prolactin is indicative of an exposure to SD and/or melatonin administration (Lincoln and Clarke 1994). This could indicate a photoperiodic effect on AQPs expression in the ovine CPs. This is in agreement with our previous observation of a higher expression of VEGFR2 and its co-receptor neuropilin 1 in the ovine CPs during SD than LD (Szczepkowska et al. 2012). Therefore it can be suggested that at least AQP1, which is involved

doi: 10.17221/6/2017-CJAS

in CSF production and is modulated by melatonin implantation, is involved in the photoperiodic modulation of CSF production in ewes.

## CONCLUSION

Our study was the first to demonstrate the AQPs expression in the ovine CP with detailing different AQP4 isoforms. Moreover, we obtained the first evidence for photoperiodic regulation of the AQPs expression, since it has been shown that melatonin implantation during LD, mimicking SD, increased the expression of AQPs on both the mRNA and protein level, what at least for AQP1 may partially explain higher TOR of CSF observed in ewes during SD.

***Acknowledgement.*** Our thanks are due to Joanna Winnicka for her technical support.

## REFERENCES

Adam C.L., Findlay P.A., Miller D.W. (2006): Blood-brain leptin transport and appetite and reproductive neuroendocrine responses to intracerebroventricular leptin injection in sheep: influence of photoperiod. Endocrinology, 147, 4589–4598.

Agre P., King L.S., Yasui M., Guggino W.B., Ottersen O.P., Fujiyoshi Y., Engel A., Nielsen S. (2002): Aquaporin water channels – from atomic structure to clinical medicine. The Journal of Physiology, 542, 3–16.

Chemineau P., Malpaux B., Delgadillo J.A., Guerin Y., Ravault J.P., Thimonier J., Pelletier J. (1992): Control of sheep and goat reproduction: use of light and melatonin. Animal Reproduction Science, 30, 157–184.

Coge F., Guenin S.P., Fery I., Migaud M., Devavry S., Slugocki C., Legros C., Ouvry C., Cohen W., Renault N., Nosjean O., Malpaux B., Delagrange P., Boutin J.A. (2009): The end of a myth: cloning and characterization of the ovine melatonin MT(2) receptor. British Journal of Pharmacology, 158, 1248–1262.

Fraser S., Cowen P., Franklin M., Francy C., Arendt J. (1983): Direct radioimmunoassay for plasma melatonin. Clinical Chemistry, 29, 386–397.

Guesdon V., Malpaux B., Delagrange P., Spedding M., Cornilleau F., Chesneau D., Haller J., Chaillou E. (2013): Rapid effects of melatonin on hormonal and behavioral stressful responses in ewes. Psychoneuroendocrinology, 38, 1426–1434.

Herman A.P., Misztal T., Herman A., Tomaszewska-Zaremba D. (2010): Expression of interleukin (IL)-1β and IL-1 receptors genes in the hypothalamus of anoestrous ewes after lipopolysaccharide treatment. Reproduction in Domestic Animals, 45, 426–433.

Herman A.P., Krawczynska A., Bochenek J., Antushevich H., Herman A., Tomaszewska-Zaremba D. (2014): Peripheral injection of SB203580 inhibits the inflammatory-dependent synthesis of proinflammatory cytokines in the hypothalamus. BioMed Research International, 2014, Article ID 475152.

Kaur C., Sivakumar V., Zhang Y., Ling E.A. (2006): Hypoxia-induced astrocytic reaction and increased vascular permeability in the rat cerebellum. Glia, 54, 826–839.

King L.S., Agre P. (1996): Pathophysiology of the aquaporin water channels. Annual Review of Physiology, 58, 619–648.

Kowalewska M., Szczepkowska A., Herman A.P., Pellicer-Rubio M.T., Jalynski M., Skipor J. (2017): Melatonin from slow-release implants did not influence the gene expression of the lipopolysaccharide receptor complex in the choroid plexus of seasonally anoestrous adult ewes subjected or not to a systemic inflammatory stimulus. Small Ruminant Research, 147, 1–7.

Lagaraine C., Skipor J., Szczepkowska A., Dufourny L., Thiery J.C. (2011): Tight junction proteins vary in the choroid plexus of ewes according to photoperiod. Brain Research, 1393, 44–51.

Li X., Kong H., Wu W., Xiao M., Sun X., Hu G. (2009): Aquaporin-4 maintains ependymal integrity in adult mice. Neuroscience, 162, 67–77.

Lincoln G.A., Clarke I.J. (1994): Photoperiodically-induced cycles in the secretion of prolactin in hypothalamo-pituitary disconnected rams: evidence for translation of the melatonin signal in the pituitary gland. Journal of Neuroendocrinology, 6, 251–260.

Misztal T., Romanowicz K., Barcikowski B. (1996): Effects of melatonin infused into the III ventricle on prolactin, beta-endorphin and luteotropin secretion in ewes during the different stages of the reproductive cycle. Acta Neurobiologiae Experimentalis, 56, 769–778.

Moe S.E., Sorbo J.G., Sogaard R., Zeuthen T., Petter Ottersen O., Holen T. (2008): New isoforms of rat Aquaporin-4. Genomics, 91, 367–377.

Nazari Z., Nabiuni M., Nejad Z.S., Delfan B., Irian S. (2015): Expression of aquaporins in the rat choroid plexus. Archives of Neuroscience, 2, e17312.

Neely J.D., Christensen B.M., Nielsen S., Agre P. (1999): Heterotetrameric composition of Aquaporin-4 water channels. Biochemistry, 38, 11156–11163.

Nesic O., Lee J., Unabia G.C., Johnson K., Ye Z., Vergara L., Hulsebosch C.E., Perez-Polo J.R. (2008): Aquaporin 1 –

doi: 10.17221/6/2017-CJAS

a novel player in spinal cord injury. Journal of Neurochemistry, 105, 628–640.

Nielsen S., Smith B.L., Christensen E.I., Agre P. (1993): Distribution of the aquaporin CHIP in secretory and resorptive epithelia and capillary endothelia. Proceedings of the National Academy of Sciences of the United States of America, 90, 7275–7279.

Oshio K., Watanabe H., Song Y., Verkman A.S., Manley G.T. (2005): Reduced cerebrospinal fluid production and intracranial pressure in mice lacking choroid plexus water channel Aquaporin-1. FASEB Journal, 19, 76–78.

Owler B.K., Pitham T., Wang D. (2010): Aquaporins: relevance to cerebrospinal fluid physiology and therapeutic potential in hydrocephalus. Cerebrospinal Fluid Research, 7, 15.

Ron N.P., Kazianis J.A., Padbury J.F., Brown C.M., McGonnigal B.G., Sysyn G.D., Sadowska G.B., Stonestreet B.S. (2005): Ontogeny and the effects of corticosteroid pretreatment on aquaporin water channels in the ovine cerebral cortex. Reproduction, Fertility and Development, 17, 535–542.

Skipor J., Thiery J.C. (2008): The choroid plexus–cerebrospinal fluid system: undervaluated pathway of neuroendocrine signaling into the brain. Acta Neurobiologiae Experimentalis, 68, 414–428.

Skowronski M.T., Lebeck J., Rojek A., Praetorius J., Fuchtbauer E.M., Frokiaer J., Nielsen S. (2007): AQP7 is localized in capillaries of adipose tissue, cardiac and striated muscle: implications in glycerol metabolism. American Journal of Physiology – Renal Physiology, 292, 956–965.

Speake T., Freeman L.J., Brown P.D. (2003): Expression of aquaporin 1 and aquaporin 4 water channels in rat choroid plexus. Biochimica et Biophysica Acta, 1609, 80–86.

Szczepkowska A., Wasowska B., Gilun P.D., Lagaraine C., Robert V., Dufourny L., Thiery J.C., Skipor J. (2012): Pattern of expression of vascular endothelial growth factor and its receptors in the ovine choroid plexus during long and short photoperiods. Cell and Tissue Research, 15, 621–628.

Thiery J.C., Robel P., Canepa S., Delaleu B., Gayrard V., Picard-Hagen N., Malpaux B. (2003): Passage of progesterone into the brain changes with photoperiod in the ewe. The European Journal of Neuroscience, 18, 895–901.

Thiery J.C., Lomet D., Schumacher M., Liere P., Tricoire H., Locatelli A., Delagrange P., Malpaux B. (2006): Concentrations of estradiol in ewe cerebrospinal fluid are modulated by photoperiod through pineal-dependent mechanisms. Journal of Pineal Research, 4, 306–312.

Thiery J.C., Lomet D., Bougoin S., Malpaux B. (2009): Turnover rate of cerebrospinal fluid in female sheep: changes related to different light-dark cycles. Cerebrospinal Fluid Research, 6: 9.

Venero J.L., Vizuete M.L., Ilundain A.A., Machado A., Echevarria M., Cano J. (1999): Detailed localization of aquaporin-4 messenger RNA in the CNS: preferential expression in periventricular organs. Neuroscience, 94, 239–250.

Venero J.L., Vizuete M.L., Machado A., Cano J. (2001): Aquaporins in the central nervous system. Progress in Neurobiology, 63, 321–336.

Wolinska E., Polkowska J., Domanski E. (1977): The hypothalamic centers involved in the control of production and release of prolactin in sheep. The Journal of Endocrinology, 73, 21–29.

Zhao S., Fernald R.D. (2005): Comprehensive algorithm for quantitative real-time polymerase chain reaction. Journal of Computational Biology, 12, 1047–1064.

Received: 2017–01–10
Accepted after corrections: 2017–10–06